Journal of Thermal Engineering
Web page info: https://jten.yildiz.edu.tr
DOI: 10.18186/thermal.1190545

Research Article

Natural ventilation in a lege space with heat source: CFD visualization and taguchi optimization

Anthati Sai CHANDRA[1], P. Nithish REDDY*[1], Harish R[2]

[1]*Department of Mechanical Engineering, Sreenidhi Institute of Science & Technology, Hyderabad, India, 500001*
[2]*School of Mechanical Engineering, Vellore Institute of Technology, Chennai, Tamilnadu, India, 600016*

ARTICLE INFO

Article history
Received: 23 November 2020
Accepted: 12 May 2021

Keywords:
Natural Ventilatio; Louvres; CFD; Heat Source

ABSTRACT

Louvre-equipped generic enclosed (LEGE) space with heat source and guiding vents is commonly seen in many buildings, heat transfer equipment and has plenty of practical applications. In the current work, natural wind- driven convection in a LEGE space system with a mono-centric heat source under five louvre configurations and different wind speeds are analyzed. The system walls are assumed adiabatic, and a heat source is introduced at the centre with five different levels of heating in the range of 100 and 400 W/m^2. The system is placed in an ample rectangular space to generate natural wind flow conditions. The efforts of conducting several experiments are reduced by applying Taguchi method and Anova is used to rank the experiments based on the responses from CFD simulations. Firstly 3D steady RANS equations are solved using the Finite volume approach where RNG k-ω the model was chosen for turbulence modelling. The Nusselt number and temperature of the heat source were noted down as responses for each case. Secondly, the percentage contribution of different factors on the temperature of heat source and optimum experiment were explored using ANOVA technique. The results are reported in contours and velocity vectors inside the enclosure, disclosing the heat flow and air circulation under different design configurations. Results show that louvres position had a maximum of 5 percent effect on the responses than other factors. From the ANOVA method, results show that the contribution of air velocity is around 80%.

Cite this article as: Chandra A S, Reddy P N, Harish R. Natural ventilation in a lege space with heat source: CFD visualization and taguchi optimization. J Ther Eng 2022;8(5):642–655.

INTRODUCTION

Natural ventilation is a method that utilizes natural forces for the circulation of air; it is mainly wind and buoyancy-driven. Natural ventilation is highly dependent on the design of inlets/exits like windows, vents, and doors [1-2]. There are specific shading devices like fins, louvres, and external roller blinds used to admit light and air but not

***Corresponding author.**
*E-mail address: dr.nithish.reddy@gmail.com

This paper was recommended for publication in revised form by Regional Editor Alibakhsh Kasaeian

Published by Yıldız Technical University Press, İstanbul, Turkey

rainwater or direct sunshine. The louvre serves as a suitable shading device that directs wind at desired magnitude and direction [3-5]. The angle of the louvre also plays an important role. Chandrashekaran et al. [6] conducted a CFD study on isolated buildings at different louvre slat angles. They concluded that the louvre slat angle of 30° and 45° enable quicker mixing of air & implementation of louvres along with natural ventilation provides lower temperature and comfort conditions. Tablada et al. [7] used external louvres and concluded that a louvre at 45° slat angles provides less air supply. Kosutova et al. [8] performed computational fluid dynamics simulation of cross- ventilation in generic isolated buildings with louvres. They concluded that the louvre slat angle of 15° is best to use because it provides enough free area for air to pass through. Several experimental analyses were done to study the influence of facade opening position and size of facade for natural ventilation in a single zone building. The difference in natural ventilation rates was due to the differences in the selection of geometric parameters, i.e. building models, size of openings, and operating inlet air velocity. Karava et al. [9] performed a wind-tunnel experiment for nine different opening positions and demonstrated flow characteristics that are essential inputs for accurate natural ventilation modelling and design. Air velocity fields in buildings were analyzed comprehensively by Tominga et al. [10].

They presented detailed experimental data and subsequent analysis of flow and dispersion similarly to Karava et al. [9]. The major conclusions from the study are; various parameters like meteorological conditions, topography, surrounding buildings, etc., play a major role in the flow and dispersion of air.Bangalee et al. [11] performed a numerical study of a one-story building with different locations of windows. The larger size of the window and increased count of windows together resulted in increased ventilation rate, which reduced ventilation time. The influence region around the structure must be modelled explicitly for predicting the ventilation flow rate accurately. Several unintended modelling errors and computing expenses can be reduced by careful design of the influence region [12-13]. Fakhrossadat et al. [14] performed a numerical analysis to study auxiliary ventilation in a coal face section of an underground mine exposed to methane gas. This ventilation system consists of a ducted exhaust fan. Their study contributed to a better understanding of the behaviour of auxiliary ventilation systems. This understanding is crucial to remove pollutant and contaminant gases from underground efficiently. Kong et al. [15] performed a comparative experimental study on the performance of stratum and mixing ventilation for space heating and concluded a decrease of 25% energy consumption and 10% improvement in indoor comfort for the same air supply parameters stratum ventilation. Tian et al. [16] included one more method i.e. dispersion ventilation for an office, and compared the obtained results. They concluded that the dispersion ventilation provides the most satisfactory comfort than others. Jiao et al. [17] performed dilution ventilation studies in the industry to reduce contaminants concentration for different cases and reported that duel inlet dilutes ventilation was more effective than single inlet dilution ventilation.

Several numerical studies were carried out using CFD to obtain detailed and clear visualization of the ventilation process and predict the best-suited model for that [18]. Ramponi et al. [19] tested 3D steady RANS approach with SST (k-ω) model and validated the results with experimental work. The effects of physical diffusion were analyzed by changing inlet profiles and grid resolution. Robert et al. [20] conducted a numerical parametric study on an existing experimental model with different positions of the vent (i) high (ii) low (iii) centre etc. The results were compared with the practical work and were in good agreement with them.

Peren et al. [21] performed CFD simulation in a generic isolated building and concluded that SST (k-ω) and RNG (k-ω) turbulent models are suitable for such studies. Ramponi et al. [22] confirmed that SST (k-ω) is also suitable for numerical ventilation analysis. The second-order discretization was able to predict indoor ventilation more accurately. Evola and Popov [23] performed computational analysis of natural wind-driven ventilation in buildings. Here Standard (K-ω) model with two equations and RNG (K-ω) turbulent models were used. The study outcomes show that results of RNG (K-ω) provide better agreement with the experimental data. But K-ω model failed near surfaces where damping impact is applicable. The parameters such as model, domain size, and boundary conditions are susceptible factors in CFD and are to be carefully chosen. Pabiouet al. [24] performed an experimental study on natural cross ventilation in a full-scale building and small-scale model. Results of both the works were compared with each other. In small-scale model flow visualization is performed and the results obtained are used as a benchmark for numerical study. Kaiser and Huges [25] performed CFD analysis on a commercial multi-directional wind tower scaled to 1:10. Different wind speeds from 0.5 m/s to 5 m/s were simulated. The smoke visualization test showed the capability of CFD in replicating airflow distribution. Bangalee and Miau [26] performed an experimental study to observe fluid-driven flow structure in natural cross-ventilation by CFD, flow visualization, and PIV measurement in 4 different cases. Results were compared among themselves. PIV measures velocity fields in different vertical planes. CFD predicts internal flow patterns and ventilation rate. Cheng and Lam [27] conducted a numerical study to investigate the effect of building wall agreements on the amount of wind-induced ventilation. The study concludes that ventilation rates are dependent on incident angles of wind.

Various numerical studies on experimental data have been performed on real-life instances. Wiriyasart and Naphon [28] conducted CFD studies to analyze the thermal distribution and air quality in a workshop with multiple heat

sources. The study concluded that temperature in workshop rooms decreased by increasing air ventilation level. Mei and Luo [29] performed a CFD study for a street canyon to determine a healthy living environment and ventilation in urban canyons. They gave the optimum design of street dimensions under isolated and vortex dominant conditions. Chang et al. [30] performed a CFD study to optimize ventilation systems in underground mines in Australia. Different duct lengths have been viewed and examined. Among the three, one with a short distance between duct outlet and facing provided the best dilution rate of DPM. Costanzo et al. [31] used a new approach combining CFD, daylighting simulation, and thermal analysis to assess natural ventilated building office thermal and visual comfort. They arrived at optimal wind-to-wall ratio values, urban aspect ratio, and floor width under different climatic conditions of Europe and North American states. O'Sullivan et al. [32] carried out ventilation studies on narrow slotted louvre systems under wind prevailing conditions. They compared the results of this louvre equipped system with that of the plain opening case, and they observed a 6.5 percent increase in air exchange rate with the louvres system compared to the plain opening case. Jiang et al. [33] developed forced convection correlations for a windward building façade with externally fitted louvres. They carried out a high-resolution simulation to compute convective heat transfer rates and Nusselt number. Pourshab et al. [34] applied horizontal and vertical louvres for an office building system in their natural ventilation studies. Numerical simulations were carried out for hot and arid climatic conditions and designed the building for optimum ventilation by reinforcing the natural airflow between the floors.

After the detailed literature survey, it was observed that the five configurations presented here and application of Taguchi, Anova, and CFD analysis is rarely attempted; this brings good advantage in handling problems of this kind. It drastically reduces the number of simulations to be conducted and reduces the computational cost. It's also effective in finding the optimum solution and the contribution of each factor. The current investigations present comprehensive finite volume analysis & optimization. Firstly, the study's main objective is to visualize using CFD and understand the ventilation process with the action of louvres under different configurations. Secondly, the effective contribution of key parameters like louvres, wind speed, and heat flux on responses in this enclosure is evaluated using ANOVA, and the best numerical experiment is identified using Taguchi.

METHODOLOGY

3D Model Configurations

Louvres are placed on one left wall (upwind) and the right wall (downwind) of the enclosure. The following are configurations chosen.

1. CC -Lovers positioned at the center on both walls
2. LL-Louvres placed low on both walls
3. HH-Louvres set high on both walls
4. HL-One louvre positioned high (left wall) and other low (right wall)
5. LH-One louvre placed low (left wall) and another high (right wall)

The location of louvres from the ground is as shown in Figure 2.

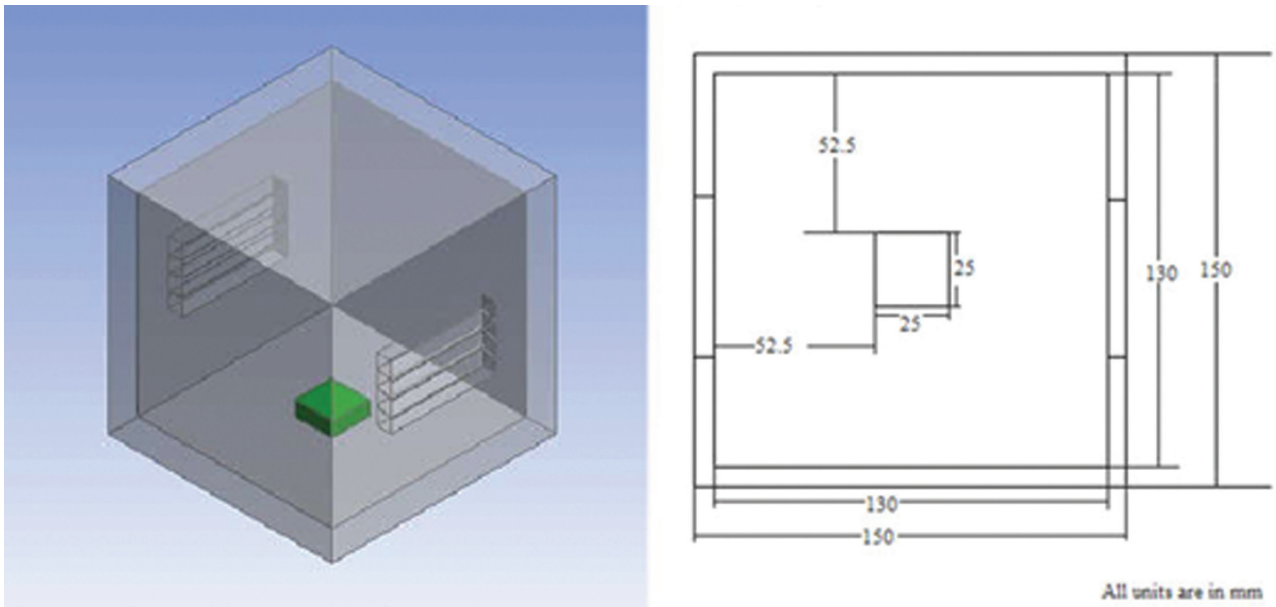

Figure 1. Geometrical model of the enclosure with a heat source.

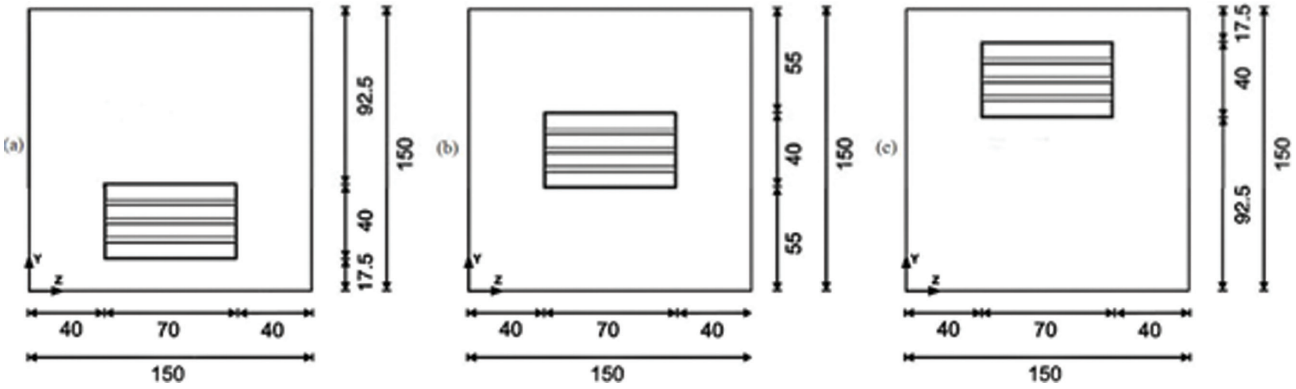

Figure 2. Position of louvre (a) low (b) center (c) high [8].

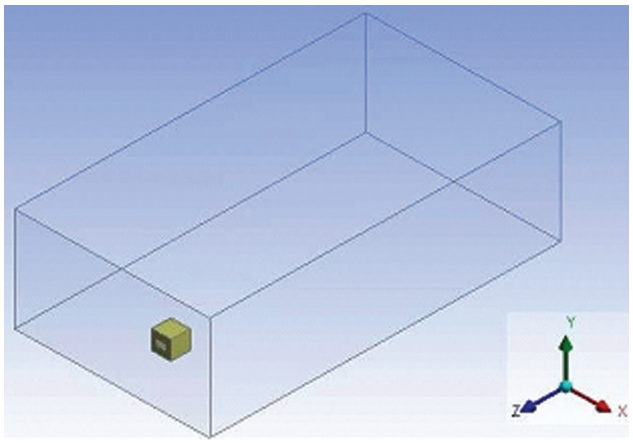

Figure 3. Computational domain.

Computational Domain and Boundary Conditions

The computational domain and setting up of boundary conditions are essential in computational fluid dynamics to solve fluid flow and heat transfer-related problems. The domain size is to be selected so that free boundary effects do not fall on flow parameters. In the present study, the size of the domain taken is 2700x1500x750 mm^3. The solid geometry with louvres which is the interest of the current study, is placed on the base of the domain, as shown in the Figure 3 . The distance from the top of the solid to the top of the domain is 750mm. The front face of the structure is placed at a distance of 450mm. The left and right spaces are 750mm each.

In the present study, the material for the fluid domain is taken as air. The inlet velocity of the air are chosen as 0.01 m/s, 0.5 m/s, 1 m/s and 2 m/s , 4 m/s, which indicate the natural wind velocities. Thermal boundary condition of constant inlet temperature (300K) was given to incoming wind. The heat flux for heat sources are 100, 150, 200, 300, and 400W/m^2. The outlet condition is specified as pressure outlet condition. Gravity is taken into consideration along the negative Y-axis and uniform wall temperatures are specified to the enclosure. No-slip condition is assumptions at walls.

Methodology

Finite volume method is used to solve the governing equations [35-36], derived from fundamental principles of heat and fluid flow. Before applying the conventional Navier-Stokes to the model in a commercial fluid dynamic solver, some necessary assumptions are made. Reynolds averaged Navier strokes equations are employed in solving the flow field and the turbulence part is modelled to calculate the Reynolds stress associated with velocity fluctua-tions. The flow is assumed steady, working fluid is treated as an ideal gas, and the properties are assumed constant. The wall temperature is kept uniform and constant at 300k that of air temp; heat transfer by radiation is neglected. A SIMPLE (Semi-Implicit Method for Pressure Linked equa-tion) algorithm is used for the pressure velocity coupling. The SIMPLE algorithm uses a relationship between velocity and pressure corrections to enforce mass conservation and to obtain the pressure field. A second-order upwind scheme is employed, and convergence is attained after all the resid-uals go below 10e-05.

Computational Mesh and Grid Independence Test

A mesh is generated as shown in the Figure 4 to apply the finite volume method at each cell centre. Meshing for the geometry near the louvres portion is done fine so that the critical effects are captured in that fi nite sp ace. The mesh for the thermal regions near the boundary must also be done fine. Face sizing and body sizing are used for the solid body to generate a very fine mesh. The various views of the mesh are shown in the Figure 4.

To establish the accuracy in CFD solutions and keep the computational cost low, it is necessary to divide the computational domain into small cells optimally. Grid size affects t he a ccuracy of o btained solution and s imulation time. The grid convergence study was performed by para-metric analysis in which parameters like maximum face

size, temperature, and velocity developed inside the cabinet are examined to determine how the mesh quality affects CFD simulation results. A grid independence test was carried out by varying the number of elements from 23500 to 17,00,000. The variation of surface temperature of the heat source is plotted against no elements, as shown in the Figure 5. It was observed that grid independence is obtained after the grid size of 4 lakh elements observed from the above Figure 5. Thus a mesh of 4.61 lakh elements is considered in the current study for better accuracy.

Validation Study

The present numerical model is validated by comparing Kosutova et al. [8] for cross-ventilation in a generic isolated building equipped with louvres. The contours of dimensionless mean velocity magnitude from the reference paper are compared with the current work in Figure 6.

RSM turbulent model was used to validate the flow contours with that of the literature [8] for this ventilation problem corresponding to the inlet velocity of 1.9m/s. Residuals limit of 10e-5 is taken for x, y, z velocities, energy, and turbulent kinetic energy for the convergence criterion. The second-order upwind discretization has opted in this implicit formulation. The results obtained are in good agreement with that of the literature [8]. The CFD model captured the flow upstream and interior of the LEGE space well and has shown decent agreement in the downstream. The minor deviations at smaller scales may be due to the approximation and mesh with that of the literature.

CFD RESULTS AND DISCUSSION

Results of thermal flow contours in the enclosed space corresponding to different geometrical and operating

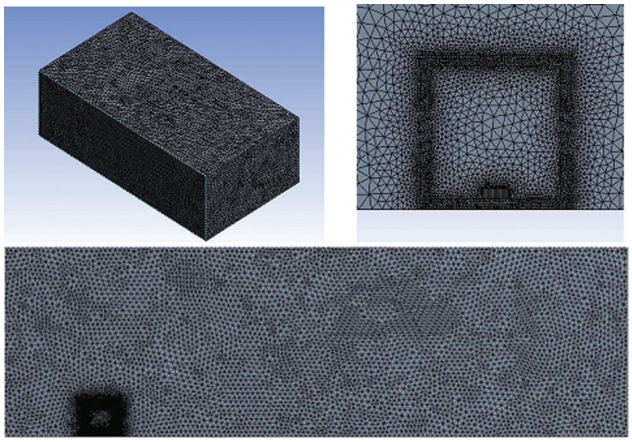

Figure 4. Computational mesh.

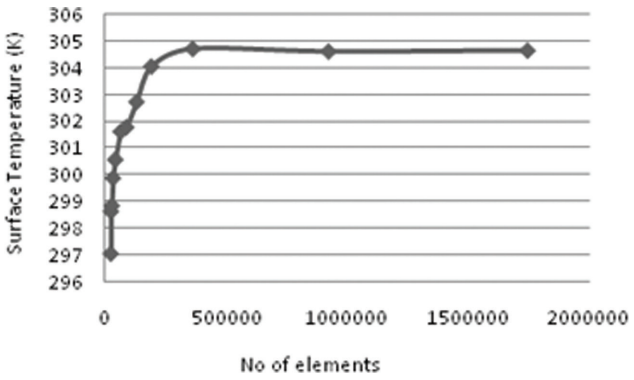

Figure 5. Grid independence test.

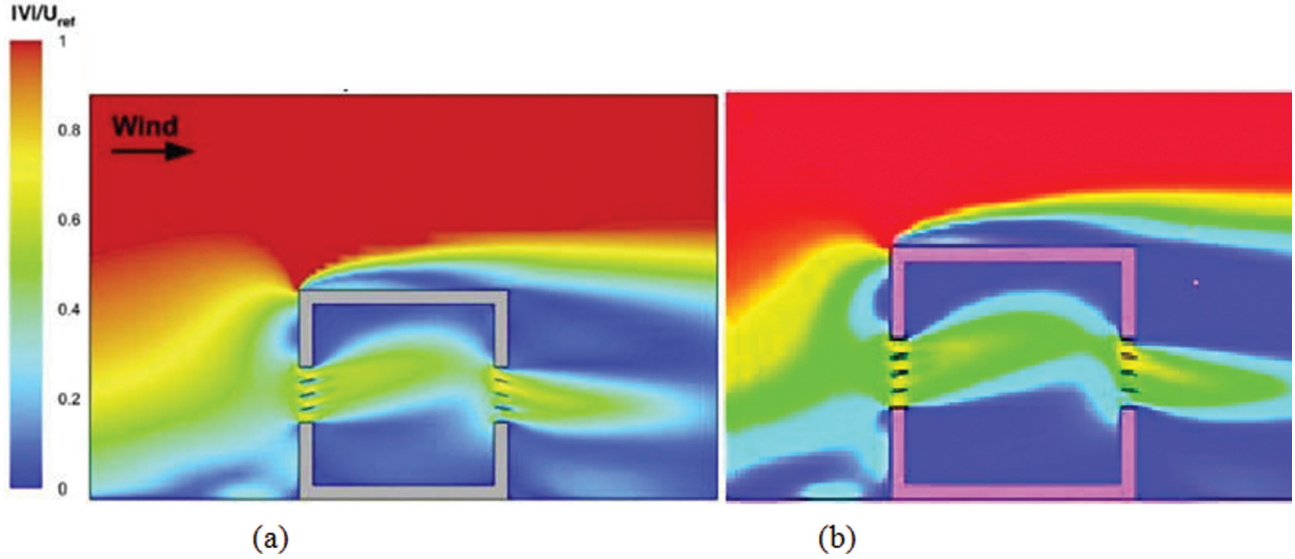

Figure 6. Comparision of contours of dimensionless mean velocity contours (a) Literature [8] (b) Present.

parameters are presented in this section. The temperature and velocity distributions and airflow patterns in the room based on different inlet air velocities, louvres, and location positions are discussed. The study case includes a monocentric heat source of the enclosure base with five different configurations of louvres, as shown in Figure 7. The five configurations chosen are (a) Louvres positioned at the centre –CC (b) Both Louvres positioned high-HH (c) Both Louvres positioned low–LL(d) Left louvre positioned high and other low- HL (e) Left louvre positioned low and right one high- LH. A heat flux boundary condition of 100 W/m^2 is specified to the heat source. Multiple numerical experiments were conducted by varying the upwind intensity, and the following interpretations are drawn. Figure 7 shows the contours of temperature and velocity contours corresponding to the upwind velocity of 0.01 m/s and heat flux = 100 W/m^2. The flow intensity is relatively high from the velocity contours in the proximity of the heat source with louvers positioned low (LL) and was relatively poor in louvers positioned high (HH). The same is directly reflected on the corresponding temperature contours of HH configuration where the heat source temperature is observed high. From the contours, it can also be understood that the heat source's hotness is felt in most portions of the enclosure in case of vent placed high (conf. b). Table 1 gives the quantitative picture of the average surface temperature on the heat source under different conditions. Firstly for minimal wind condition i.e., for inlet air velocity of 0.01 m/s and the heat flux value of 100 W/m^2, the average temperature on the surface of the heat source was found maximum for configuration (b) with 327.17 K. The temperature was observed minimum for louvers positioned low (configuration-c) with 313.3 K followed by configuration (e). From velocity contours, the circulation of air in the enclosure is found more of less throughout in case of configurations a and d. But the temperature of the heat source was found slightly higher in case d. This result shows the warmness of the heat source was felt in most regions of the enclosure with a lower circulation rate, and this happened when vents were placed high. Internal air circulation was more uniform with configurations a and d.

The same experiment is repeated for further higher wind flow rates. Figure 8 & Figure 9 show the contours of temperature and velocity corresponding to the upwind velocity of 1 m/s and 4 m/s, respectively for heat flux = 100 W/m^2. For air velocity of 1 m/s, the temperature is maximum with 303.87 K (ref. Table 1) for louvers positioned high and is low for louvers positioned low with 301.73 K. Interestingly, with further increase in air velocity to 2 and 4 m/s, the same trend is observed but the margin of difference in higher and lower temperatures has decreased. The maximum and minimum temperatures observed are 302.48 K and 301.09 K, respectively, for 2 m/s.

In case of 4m/s wind flow temperature was maximum and minimum for case with louvers positioned high and low with 301.52 K and 300.72 K, respectively. This trend may be because of the variation in the degree of convection currents within the enclosure for different configurations with change in wind speed. The sensitivity of surface temperature of heat source to wind velocity got minimized with an increase in wind flow rate. Such a phenomenon can

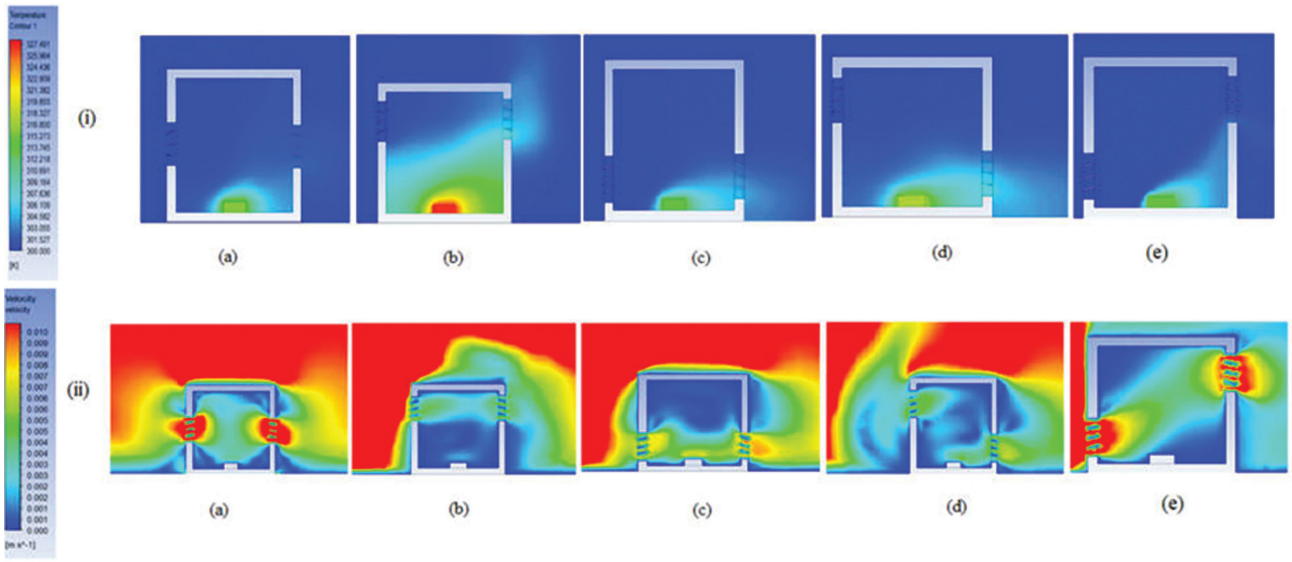

Figure 7. (i) Temperature and (ii) Velocity contours corresponding to upwind velocity of 0.01 m/s and Heat flux = 100 W/m2
(a) Louvres positioned at center (b) Louvres positioned high (c) Louvres positioned low (d) One louvre positioned at high and other low (e) One louvre positioned at low and other high.

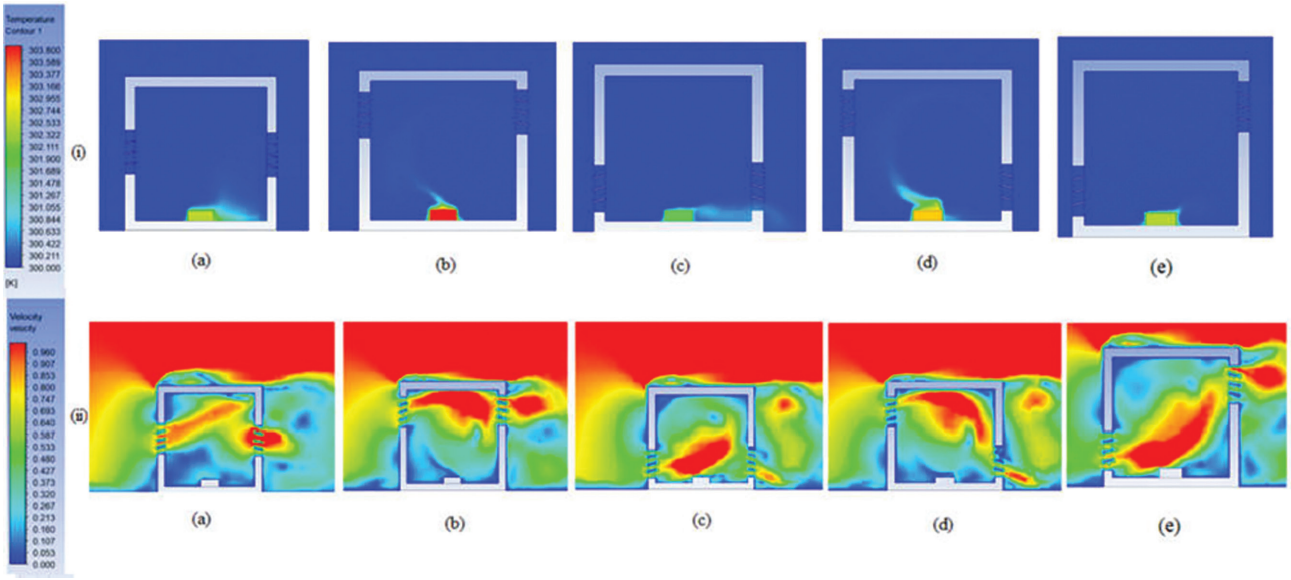

Figure 8. Temperature and Velocity contours at upwind velocity of 1 m/s
(a) Louvres positioned at center (b) Louvres positioned high (c) Louvres positioned low (d) One louvre positioned at high and other low (e) One louvre positioned at low and other high.

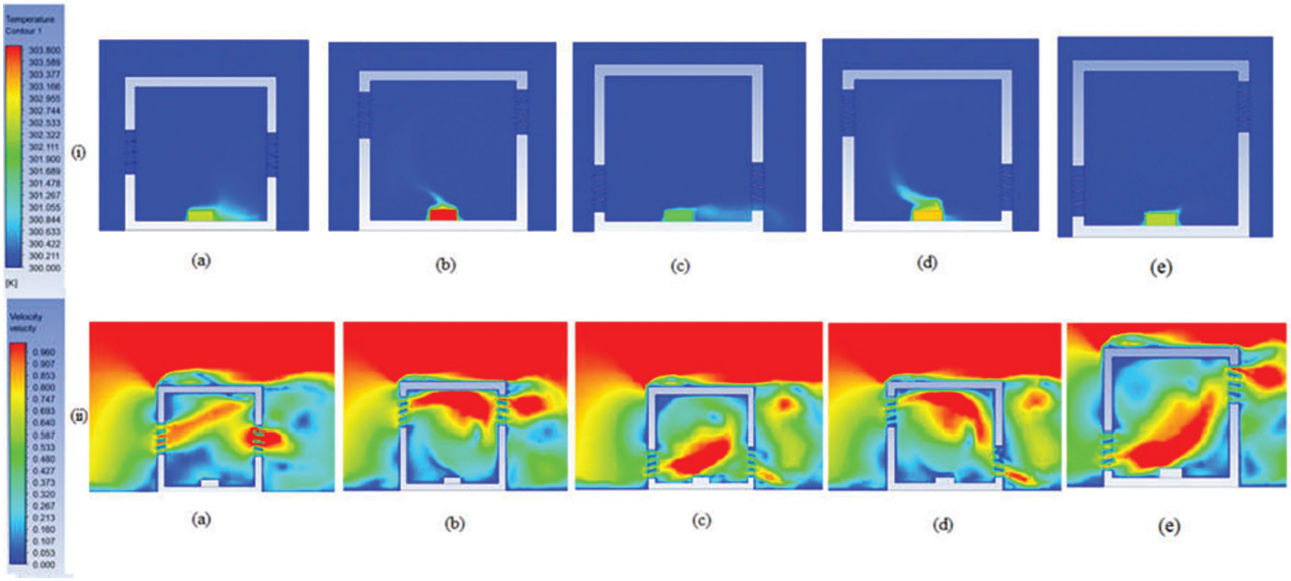

Figure 9. Temperature and Velocity contours at upwind velocity of 4 m/s
(a) Louvres positioned at center (b) Louvres positioned high (c) Louvres positioned low (d) One louvre positioned at high and other low (e) One louvre positioned at low and other high.

be better understood from the velocity vectors. Figure 10 represents velocity vectors inside the enclosed space for different wind velocities. The convection currents generated within the enclosure are observed low at 0.01m/s or minimum wind conditions and augmented with an increase in wind velocity. For louvers positioned low& LH configurations, there are direct convection currents over the heat sources, which results in more heat transfer rate. For louvers positioned at high (HH) and high-low positions, relatively weak secondary convection currents participated in convective heat transfer from the heat source. Thus the heat transfer rates were low. These have a direct effect on the temperature and Nusselt number of the heat source. Table 1 shows the details about the steady-state temperature of

the heat source in each case at different wind velocities, whereas Table 2 shows the corresponding Nusselt numbers. The stronger strength of convection currents near the heat source in the low-low (LL) approach resulted in higher Nu and lower temperature, whereas in the case of high-high (HH) configuration, the strength of vectors is low near heat source resulting in higher surface temp and lower Nusselt number.

Calculation of Nusselt number (Nu):

$$Q = h\ As\ (Ts - T\infty) \quad (1)$$

$$Nu = h\ L/k \quad (2)$$

Where, free stream temperature T∞ = 300 K; Surface area As = 6.25x10e-4 m^2; h = Convection Heat Transfer

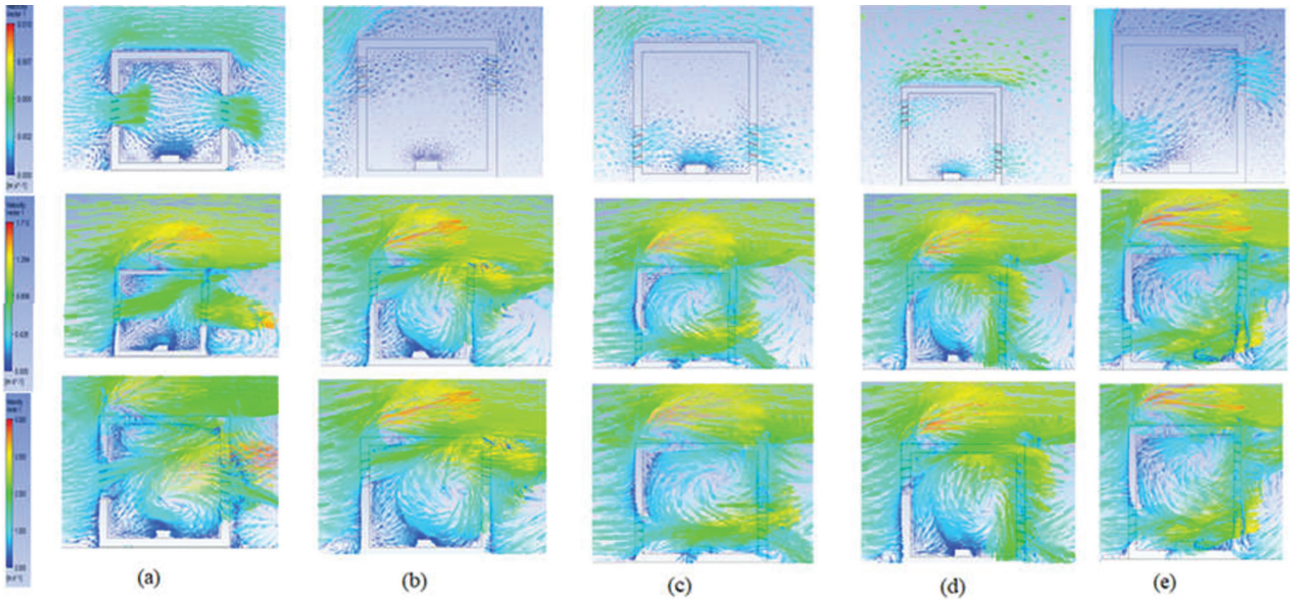

Figure 10. Velocity vectors at different wind velocities 0.01 m/s, 1 m/s, 4m/s (top to bottom)
(a) Louvres positioned at center (b) Louvres positioned high (c) Louvres positioned low (d) One louvre positioned at high and other low (e) One louvre positioned at low and other high.

Table 1. Average surface temperature of heat source

Position of Louvres	Velocity (m/s)	0.01	0.5	1.0	2.0	4.0
Centre (CC)		315.532	304.032	302.524	301.463	300.942
Low (LL)		313.305	302.681	301.728	301.091	300.725
High (HH)		327.174	306.072	303.870	302.480	301.523
High-Low(HL)		317.356	304.737	303.146	301.928	301.200
Low-High(LH)		314.004	303.081	301.923	301.332	300.826

Table 2. Nusselt number for heat source

Position Of Louvres	Velocity (m/s)	0.01	0.5	1.0	2.0	4.0
Centre (CC)		5.983	23.397	37.517	64.688	100.452
Low(LL)		7.010	35.317	54.736	86.707	130.558
High (HH)		3.369	15.476	24.376	38.082	62.140
High Low (HL)		5.334	19.913	29.984	49.008	78.811
Low High (LH)		6.635	30.618	49.242	71.093	114.644

Coefficient; L = Characteristic Length; k = Thermal Conductivity of the Fluid.

TAGUCHI METHOD & ANOVA

Design of experiments

To improve experiments design and analyze the system thoroughly, an optimization study was carried out. Taguchi method was used to design experiments and performed various analyses to understand the relative contribution of each parameter. ANOVA–Analysis of variance technique is applied. This is the statistical method used to test differences between two or more means. This method has got the name as it is analyzing variance.

For optimization, we consider three controllable factors like air velocity, heat flux, and position of louvers and two uncontrollable factors - Nusselt number and temperature with 5 levels (ref Table 3).

Table 4 shows the set of meaningful experiments designed by Taguchi method. The corresponding two uncontrollable factors are obtained using CFD simulations. Table 5 gives design summary of Taguchi array where a number of factors is 3 and runs are 25. Table 6 gives the corresponding signal to noise ratio data. From the table, air velocity is more influencing factor on Nusselt number and position of louvers had the next best role to

Table 3. Table of controllable factors

Air velocity(m/s)	Heat Flux(W/m^2)	Configuration of Louvres(mm)
0.01	100	1
0.5	150	2
1	200	3
2	300	4
4	400	5

Table 4. Set of twenty five Taguchi experiments and their corresponding Nusselt number and temperature values obtained from previous CFD studies

S.NO	Velocity (m/s)	Heat flux (W/m2)	Louvres Configuration	Nu	Temperature (K)
1	0.01	100	1	5.983	315.532
2	0.01	150	2	1.871	337.039
3	0.01	200	3	2.753	333.619
4	0.01	300	4	2.483	353.830
5	0.01	400	5	2.643	367.534
6	0.50	100	2	15.476	306.072
7	0.50	150	3	18.057	303.987
8	0.50	200	4	10.575	309.091
9	0.50	300	5	14.587	309.882
10	0.50	400	1	12.892	314.916
11	1.00	100	3	54.736	301.728
12	1.00	150	4	15.791	304.559
13	1.00	200	5	22.564	304.261
14	1.00	300	1	19.690	307.321
15	1.00	400	2	12.995	314.798
16	2.00	100	4	49.008	301.928
17	2.00	150	5	34.917	302.062
18	2.00	200	1	32.848	302.927
19	2.00	300	2	19.787	307.285
20	2.00	400	3	36.954	305.286
21	4.00	100	5	114.644	300.826
22	4.00	150	1	47.459	301.517
23	4.00	200	2	31.586	303.044
24	4.00	300	3	71.327	302.021
25	4.00	400	4	34.793	305.527

play. However,, the SN ratio analysis showed that louvers' position has a relatively lower influence o n t he N usselt number and stood rank 3. The same ranks are also shown in the Means Table 7.

Similarly, Table 8 & Table 9 are response tables for SN ratio and means concerning temperature vs. controllable factors. These tables also predict that the air velocity has a higher influence on the surface temperature in a reciprocal manner. The r anks r emained t he s ame e ven h ere as that of for another uncontrollable parameter Nusselt number.

Figure 11 & Figure 12 gives a graphical representation of the means of Means and SN ratio plots corresponding to Table 6-9. Table 10 gives the percentage contribution of each controllable factor obtained by analysis of variance. ANOVA results show that the contribution of Air velocity over uncontrollable factor Nusselt number as 89.81 %, which is very high, followed by the position of Louvres (6.89%) and finally the least contribution from heat fl ux (3.09%).

Table 11 gives the calculations and contributions in regard to temperature. Here, it is observed that Air velocity has a maximum contribution of 70.48% and then followed by louvers 9.20%. The heat flux has shown as less as 9.20% influence over the temperature.

Anova

From Taguchi optimization technique, the optimized parameter values of our experiments are Air velocity 4.0 m/s, Heat flux 100 w/m^{2}and LH configuration of louvres. From the set of twenty-five experiments, experiment no. 21 was found optimum.

By using the above ANOVA method[37,38] the contribution of air velocity is around 87% and position of louvres has a contribution of 5.13% in the case of Nusselt number and 78.35%, 2.98% respectively in case of surface temperature. Therefore we can conclude that air velocity is an important parameter and heat flux has considerable influence. The position of louvers had a maximum of 5.13% influence on the Nusselt number.

Table 5. Design summary

Taguchi Array	L25(5^3)
Factors:	3
Runs:	25

Table 6. Response table for signal to noise ratios for Nusselt Number (larger the better)

Level	Air Velocity(m/s)	Heat Flux(w/m2)	Position Of Louvres(mm)
1	9.223	29.818	25.497
2	22.979	23.786	21.486
3	26.792	23.334	27.423
4	30.455	24.011	23.398
5	34.520	23.021	26.167
Delta	25.296	6.796	5.937
Rank	1	2	3

Table 7. Response table for means: Nusselt number

Level	Air Velocity(m/s)	Heat Flux(w/m2)	Position Of Louvres(mm)
1	3.147	47.969	23.774
2	14.317	23.619	16.343
3	25.155	20.065	36.765
4	34.703	25.575	22.530
5	59.962	20.055	37.871
Delta	56.815	27.914	21.528
Rank	1	2	3

Table 8. Response table for signal to noise ratios: Surface temperature (Smaller the better)

Level	Air Velocity(m/s)	Heat Flux(w/m2)	Position Of Louvres(mm)
1	-50.66	-49.69	-49.78
2	-49.79	-49.81	-49.92
3	-49.73	-49.84	-49.80
4	-49.65	-49.98	-49.95
5	-49.62	-50.13	-49.99
Delta	1.04	0.43	0.21
Rank	1	2	3

Table 9. Response table for means: Surface temperature

Level	Air Velocity(m/s)	Heat Flux(w/m2)	Position Of Louvres(mm)
1	341.5	305.2	308.4
2	308.8	309.8	313.6
3	306.5	310.6	309.3
4	303.9	316.1	315.0
5	302.6	321.6	316.9
Delta	38.9	16.4	8.5
Rank	1	2	3

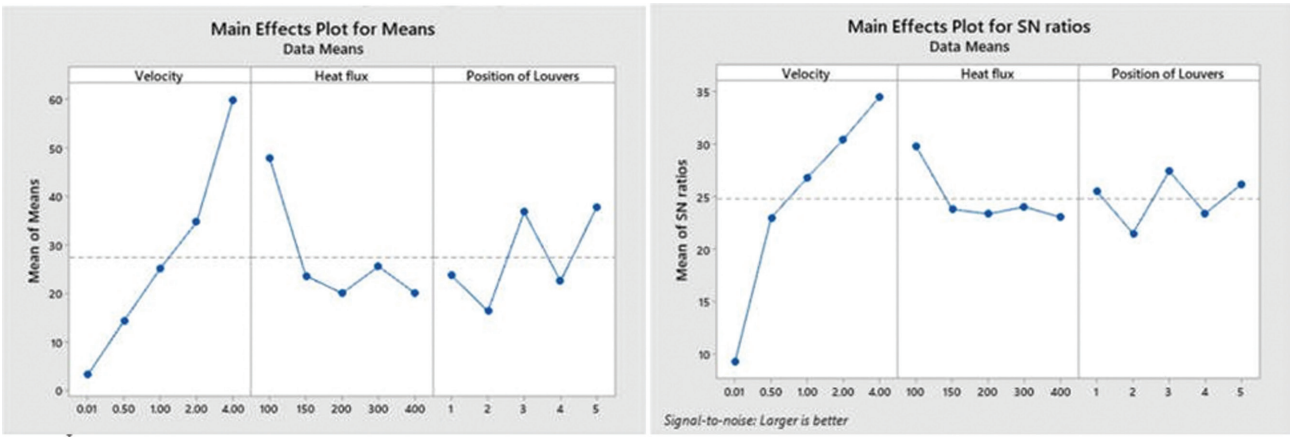

Figure 11. Mean of means and SN ratio plot for Nusselt number.

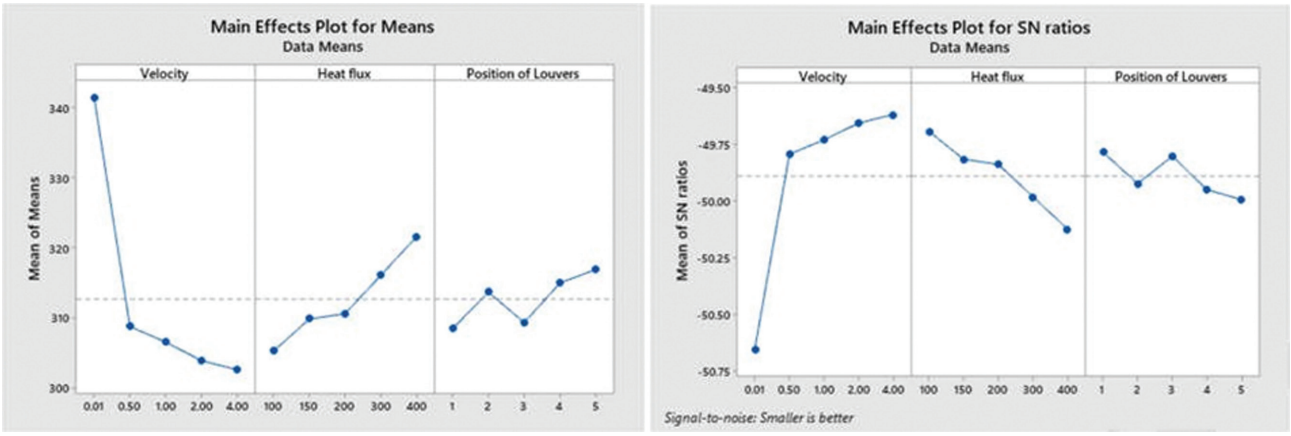

Figure 12. Mean of means and SN ratio plot for Surface Temperature.

Table 10. Analysis of variance for transformed response : Nusselt Number

Source	DF	Seq SS	Contribution	Adj SS	Adj MS	F-Value	P-Value
Air Velocity(m/s)	4	24.9432	87.03%	24.9432	6.23581	633.95	0.000
Heat Flux(w/m2)	4	2.1302	7.43%	2.1302	0.53254	54.14	0.000
Position Of Louvres(mm)	4	1.4703	5.13%	1.4703	0.36759	37.37	0.000
Error	12	0.1180	0.41%	0.1180	0.00984		
Total	24	28.6618	100.00%				

Table 11. Analysis of variance for transformed Rresponse :Surface temperature

Source	DF	Seq SS	Contribution	Adj SS	Adj MS	F-Value	P-Value
Air Velocity(m/s)	4	4006.3	78.35%	4006.3	1001.57	32.52	0.000
Heat Flux(w/m2)	4	584.9	11.44%	584.9	146.22	4.75	0.016
Position Of Louvres(mm)	4	152.6	2.98%	152.6	38.15	1.24	0.346
Error	12	369.6	7.23%	369.6	30.80		
Total	24	5113.3	100.00%				

CONCLUSION

The study presents a detailed analysis of natural ventilation in a louver-equipped generic enclosed space using CFD and Taguchi–ANOVA methods. Numerical Taguchi experiments were designed and carried out for five different Louvre configurations. The results obtained from CFD simulations are analyzed and ranked later using ANOVA. The temperature and velocity variation under different wind speeds are presented, and also a variation of heat dissipation inside the enclosure has been investigated and tabulated. Based on the results following conclusion was made.

- The flow in the enclosure is dominated by the wind passing through the vents
- Effective driving away of heat from the mono-centric source was achieved in louvres positioned low (LL) followed by LH, CC, HL, and HH configurations.
- In the case of LL and LH, relatively direct primary convection currents acted, whereas in other cases, the relatively weak secondary convection currents participated.
- Lower thermal sensitivity is observed for louvers positioned low when compared to other configurations. The temperature variation on heat source corresponding to changes in wind speed from 0.5 m/s to 1m/s, 2 m/s to 4m/s were reported as 1.12% and 0.26%, respectively.
- At higher wind velocities, the sensitivity of heat source temperature has decreased irrespective of Louvre positions.
- A minimal influence of louvre on-air exchange is observed in the case of louvres positioned high.
- A set of designed twenty-five TAGUHI experiments are conducted, and the twenty-first experiment was reported optimum with optimized parameters of air velocity 4.0 m/s, Heat flux 100 w/$m^{2,}$ and LH Louvre configuration.
- From the ANOVA method, results show that the contribution of air velocity is around 78-87% on the advection phenomenon and the position of louvers has the least contribution of about 5%.

FUTURE SCOPE

There is a scope in developing the natural ventilation in the space by experimenting with multiple heat sources. Even interchanging the heat sources position may also be considered to provide the optimal position to provide a better ventilation rate. Increasing the number of inlets and outlets for air to two may be considered. Further, their position can also be varied.

NOMENCLATURE

Roman symbols

H	Height of the building, [m]
I	Turbulence intensity, [%]
k	Turbulent kinetic energy, [m^2/s^2]
v	Instantaneous velocity component in y direction
w	Instantaneous velocity component in z direction
x	Horizontal coordinate, [m]
y	Vertical coordinate, [m]
y0	Aerodynamic roughness length, [m]

Greek symbols

ε	Turbulence dissipation rate, [m^2/s^3]
ν	Kinematic viscosity [m^2/s]
ω	Specific dissipation rate, [1/s]
ρ	Density, [kg/m^3]
α	Thermal diffusivity, [m^2/s]

Acronyms

RANS	Reynolds averaged Navier-Stokes
CFD	Computational fluid dynamics
RNG	Renormalization group
RSM	Reynolds stress model
SIMPLE	Semi implicit method for pressure linked equations
SST	Stress-shear transport
ANOVA	Analysis of variance
PIV	Particle image velocimetry

Configurations

LL	Low-Low
LH	Low-High
HL	High-Low
HH	High-High
CC	Centre-Centre

AUTHORSHIP CONTRIBUTIONS

Authors equally contributed to this work.

DATA AVAILABILITY STATEMENT

The authors confirm that the data that supports the findings of this study are available within the article. Raw data that support the finding of this study are available from the corresponding author, upon reasonable request.

CONFLICT OF INTEREST

The author declared no potential conflicts of interest with respect to the research, authorship, and/or publication of this article.

ETHICS

There are no ethical issues with the publication of this manuscript.

REFERENCES

[1] Cheng Z, Li L, Bahnfleth WP. Natural ventilation for gymnasia- a case study of ventilation and comfort in a multisport facility in north eastern US. Build Environ 2016;108:85–98. [CrossRef]

[2] Salah H, Safaa A, Kadhum A. Experimental and numerical investigation of convection heat transfer in an enclosure with a vertical heated block and baffles. J Therm Eng 2021;7:367–386.

[3] Oztop HF, Selimefendigil F, Abu-Nada E, Al-Salem K. Recent developments of computational methods on natural convection in curvilinear shaped enclosures. J Therm Eng 2016;2:693– 698. [CrossRef]

[4] Cheng-Hu H, Ohba M, Kurabuchi T. Numerical study of cross-ventilation using two equations Reynolds- Averaged Navier- Stokes. Int J Ventil 2016;4:123–132.

[5] Ahmed NA, Wongpanyathaworn K. Optimizing louvre location to improve indoor thermal comfort based on natural ventilation. Proced Eng 2012:49:169–178. [CrossRef]

[6] Chandrashekaran D. Airflow through louvreed openings effect of louvre slats on air movement inside a space. University of Southern California dissertations and theses 2010. https://doi.org/10.25549/USCTHESES-M3426

[7] Tablada A, Carmeliet J, Baelmans M, Saelens D. Exterior louvres as a passive cooling strategy in a Residential Building: Computational Fluid Dynamics and building energy simulation modeling. 26th Conference on Passive and Low Energy Architecture, Quebec City, Canada, 22-24 June 2009.

[8] Kosutova K, Hooff TV, Vanderwel C, Blocken B, Hensen J. Cross-ventilation in a generic isolated building equipped with louvres: Wind-tunnel experiments and CFD simulations. Build Environ 2019;154:263–280. [CrossRef]

[9] Karava P, Stathopoulos T, Athienitis AK. Air flow assessment in cross-ventilated buildings with operable facade elements. Build Environ 2011;46:266–279. [CrossRef]

[10] Tominga Y, Blocken B. Wind tunnel analysis of flow and dispersion in cross-ventilated isolated buildings: Impact of opening positions. Wind Eng Indust Aerodynamics 2016;155:74–88. [CrossRef]

[11] Bangalee MZI, Miau JJ, Lin S, Ferdows M. Effects of lateral window position and wind direction on wind-driven natural cross ventilation of a building: a computational approach. J Comput Eng 2014;2014:310358. [CrossRef]

[12] Tong Z, Chen Y, Malkawi A. Defining the influence region in neighborhood- scale CFD simulations for natural ventilation design. Int J Appl Energy 2016;182:625–633. [CrossRef]

[13] Amores CP, Mazarron FR, Canas I, Saez PV. Natural Ventilation analysis in an underground construction: CFD simulation and experimental validation. Tunnelling Underground Space Technol 2016;90:162–173. [CrossRef]

[14] Fakhrossadat H, Bagherpour R, Saiied MA. Numerical simulation of methane distribution in development zones of underground coal mines equipped with auxiliary ventilation. Tunneling Underground Space Technol 2019;89:68–77. [CrossRef]

[15] Kong X, Xi C, Li H, Lin Z. A comparative experimental study on performance of mixing ventilation and stratum ventilation for space heating. Build Environ 2019;157:34–46. [CrossRef]

[16] Tian X, Li B, Ma Y, Liu D, Li Y, Cheng Y. Experimental study of local thermal comfort and ventilation performance for mixing, displacement and stratum ventilation in an office. Sustain Cities Soc 2019;50:101630. [CrossRef]

[17] Jiao Z, Yuan S, Ji C, Mannan MS, Wang Q. Optimization of dilution ventilation layout design in confined environments using Computational Fluid Dynamics (CFD). Loss Prevention Process Indust 2019;60:195–202. [CrossRef]

[18] Popovici CG. HVAC system functionality simulation using ANSYS- FLUENT. Sustainable Solutions for Energy and Environment, EENVIRO 2016. [CrossRef]

[19] Ramponi R, Blocken B. CFD simulation of cross-ventilation for a generic isolated building: Impact of computational parameters. Build Environ 2012;53:34–48. [CrossRef]

[20] Moroney RN. CFD prediction of airflow in buildings for natural ventilation, 11th America's Conference on Wind Engineering 2009.

[21] Peren JI, Van Hooff T, Leite BCC, Blocken B. CFD analysis of cross ventilation of a generic isolated building with asymmetric opening positions impacts roof angles and opening position. Build Environ 2014;85:263–276. [CrossRef]

[22] Ramponi R and Blocken B. CFD simulation of cross ventilation for generic isolated building: impact of computational parameters. Build Environ 2012;53:34–48. [CrossRef]

[23] Evola G, Popov V. Computational analysis of wind driven natural ventilation in buildings. Energy Build 2006;38:491–501. [CrossRef]

[24] Pabiou H , Salort J, Chilla F, Menezo C. Natural cross ventilation of buildings, an experimental study. 6th International Building Physics Conference, IBPC 2015. [CrossRef]

[25] Calautit JK, Hughes BR. Wind tunnel and CFD study of natural ventilation performance of a commercial multi-directional wind tower. Build Environ 2015;80:71–83. [CrossRef]

[26] Bangalee MZI, Miau JJ , Lin SY, Yang JH. Flow visualization, PIV measurement and CFD calculation for fluid driven cross ventilation in a scale model. Energy Build 2013;66:306–314. [CrossRef]

[27] Cheng CCK, Lam KM. Effects of building wall arrangements on wind induced ventilation through the refuge floor of a tall building. Wind Eng Indust Aerodynamics 2008;96:656–664. [CrossRef]

[28] Wiriyasart S, Naphon P. Numerical study on air ventilation in the workshop room with multiple heat sources. Case Stud Therm Eng 2019;13:100-405.

[29] Mei SJ and Luo Z. Street canyon ventilation and air bone pollutant dispersion: 2D versus 3D CFD simulation. J Sustain Cities Soc 2019;50:101700. [CrossRef]

[30] Chang P, Xu G , Zhou F , Mullins B, Abhishek S. Minimizing DPM pollution in an underground mine by optimizing auxiliary ventilation systems using CFD. Tunneling Underground Space Technol 2019;87:112–121. [CrossRef]

[31] Costanzo V, Donn M, Thermal and visual comfort assessment of natural ventilated office buildings in Europe and North America. Energy Build 2017;140:210–223. [CrossRef]

[32] O'Sullivan PD, Kolokotroni M. A field study of wind dominant single sided ventilation through a narrow slotted architectural louvre system. Energy Build 2017;138:733–747. [CrossRef]

[33] Jiang F,Yuan Y ,Li Z, Zhao Q, Zhao K. Correlations for the forced convective heat transfer at a windward building façade with exterior louvre blinds. Solar Energy 2020;209:709–723. [CrossRef]

[34] Pourshab N, Tehrani MD , Toghraie D , Rostami S. Application of double glazed facades with horizontal and vertical louvres to increase natural air flow in office buildings. Energy 2000;200:117486. [CrossRef]

[35] Alfonsi G. Reynolds averaged navier stokes equations for turbulence modeling. Appl Mech Rev 2009;62:040802. [CrossRef]

[36] Quarteroni A. Navier-Stokes equations. MS& A 2017; 457-510. [CrossRef]

[37] Lesik SA. Applied Statistical Inference with MINITAB. London: Chapman and Hall Press; 2019;2:230–340. [CrossRef]

[38] Cryer JD, Ryan BF, Joiner BL. MINITAB (R) Handbook. International edition Brooks/Cole publications 2012;6:98–180.